Optical rotary echoes

N. C. Wong, Satoru S. Kano, and Richard G. Brewer
IBM Research Laboratory, San Jose, California 95193
and Department of Applied Physics, Stanford University, Stanford, California 94305
(Received 9 August 1979)

The first observation of optical rotary echoes, the optical analog of rotary spin echoes, is reported. Rotary echoes are produced in a quantum-mechanical two-level system which is driven resonantly (nutation effect) by a coherent field that suffers a sudden phase retardation. The initial nutation transient dephases, because of an inhomogeneity in either the driving field or the transition frequency of the sample, and then rephases to form an echo following the phase-shifting pulse. Hence, optical rotary and photon echoes are similar processes—the former being an interference in nutation and the latter an interference in free precession. Perturbative solutions of the Bloch equations are derived for the case where inhomogeneous dephasing arises from Doppler broadening and the Rabi frequency exceeds the homogeneous damping rate. Observations of the optical rotary echo in I_2 vapor are facilitated by the technique of laser frequency switching, which generates precise phase shifts in the optical field. The measurements corroborate detailed theoretical predictions.

I. INTRODUCTION

In 1959 Solomon[1] reported a new coherent transient effect in nuclear magnetic resonance (NMR) —*rotary spin echoes*. While this phenomenon resembles the usual spin echo,[2] important differences exist which make it particularly useful in the measurement of long relaxation times. Whereas the spin echo is a manifestation of free induction decay[3] (FID) and appears in the absence of a driving field, the rotary echo is a manifestation of spin nutation[4] and appears in the presence of a driving field. In this article we report observations and a theory of *optical rotary echoes*, which are the optical analog of rotary spin echoes.

A Bloch-vector-model[5] description of rotary spin echoes (Fig. 1) provides a simple introduction to the subject. Consider a two-level spin system in the rotating frame where a static magnetic field H_0 lies along the z axis and a radio frequency field H_1 lies along the x axis. We presume for the moment, as Solomon did, that the inhomogeneity in H_1 is much larger than that in H_0 and thus determines the spin-nutation decay rate. In other words, the distribution in the Rabi frequency is much larger than the static inhomogeneous broadening. Here and in the discussion which follows, assume the rf pulse sequence shown in Fig. 2, where the rf frequency Ω', which is initially out of resonance with the spin system, comes into resonance at time $t=0$ owing to the frequency switch $\Omega' \rightarrow \Omega$. This pulse causes a magnetization M, which is assumed to be directed along the $-z$ axis at $t=0$, to precess in the yz plane about the x axis, where the angle of precession in time T is $\theta=\gamma H_1 T$. For an inhomogeneous distribution in H_1 the magnetization vectors will precess at different rates and therefore through different angles θ, causing them to get out of phase.

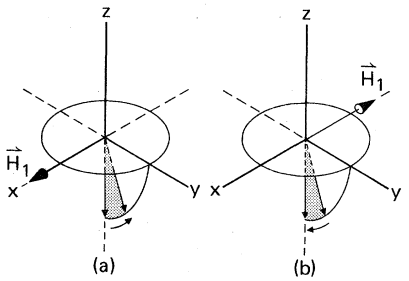

FIG. 1. Bloch-vector description of rotary echoes showing evolution of magnetization vectors M before and after the phase interruption. (a) The M vectors nutate at different rates in the initial direction and dephase. (b) After $\vec{H}_1$ field reverses its direction, the M vectors nutate at same rates as before but in the opposite direction and rephase to form an echo.

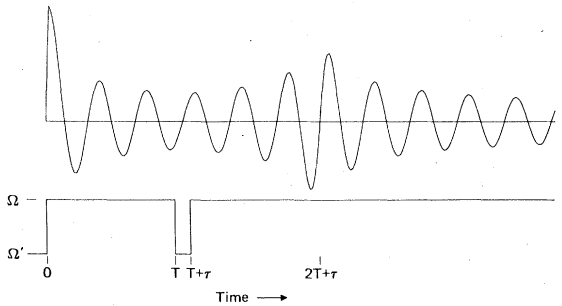

FIG. 2. Lower curve: laser frequency switching pulse sequence for rotary echoes; upper curve: computer plot of the transient response showing nutation signal and rotary echo formed at $t=2T+\tau$.

Now assume that at time $t=T$ the rf frequency is switched out of resonance, $\Omega \to \Omega'$, for a duration τ, so that the rf field suffers a phase change

$$\phi = (\Omega' - \Omega)\tau .$$

For the case $\phi = \pi$ the direction of H_1 in the rotating frame is reversed. At the end of the pulse at $t = T + \tau$, the switch $\Omega' \to \Omega$ brings the rf field back into resonance with the spins, and they begin to execute precessional motions about the x axis in the opposite direction but at the same rate as before. The phase interruption thus acts as a mirror which reflects the initial nutation signal backward in time. Therefore at time $t = 2T + \tau$ all magnetization vectors will appear in phase along the $-z$ axis, producing an echo. A computer plot of this dephasing-rephasing behavior (see Sec. II for details) is shown also in Fig. 2.

It will be evident from the above argument that an rf phase shift of $\phi = 0$ or 2π will not affect the spins, and consequently the echo amplitude will be zero. In general we can see that the

$$\text{echo amplitude} = \begin{cases} \text{a maximum}, & \phi = \pi, 3\pi, 5\pi, \ldots \\ 0, & \phi = 0, 2\pi, 4\pi, \ldots . \end{cases} \tag{1.1}$$

Solomon noted that for liquids the envelope function of a rotary echo will be characterized by an exponential decay rate α, which is the average value of the longitudinal and transverse components:

$$\alpha = \tfrac{1}{2}(1/T_1 + 1/T_2) . \tag{1.2}$$

Furthermore, using a multiple-pulse sequence consisting of π-phase-shift pulses, he showed that dephasing arising from self-diffusion can be minimized and very long dephasing times measured because errors in the π-phase-shift pulses are not cumulative, as in a Carr-Purcell[6] experiment.

The possibility of observing optical rotary echoes had been suggested by Nurmikko and Schwarz,[7] and such an effect has been detected recently in the microwave region by Rohart *et al.*[8] for a molecular rotational transition, using the method of Stark switching.[9]

Optical rotary echoes are observed here for the visible transition of I_2 using laser frequency switching.[10] This technique is ideally suited for producing well-defined phase shifts in a coherent light wave, making the observation of optical rotary echoes a simple matter. In contrast to earlier NMR[1] and microwave[7] studies, our measurements are performed in the low-intensity regime where the Rabi frequency is much smaller than the Doppler linewidth. The nature of the solutions to the Bloch equations for both low- and high-intensity limits is derived for an inhomogeneously broadened optical transition subject to population decay and homogeneous dephasing processes. We see that essentially all of the characteristics described above for NMR apply to the optical region as well.

II. THEORY

A. Equations of motion

It is not immediately evident that the optical rotary echo is described by the same theoretical treatment which has been applied in NMR.[1,11] For example, at optical frequencies, inhomogeneous broadening is often the dominant line-broadening mechanism, the transition levels relax to a multilevel reservoir, and spontaneous radiative decay is usually important. However, for spins, the lines are frequently homogeneously broadened, there often are only two spin states, and spontaneous decay can be ignored. These differences have prompted us to carry out a detailed calculation using the Bloch equations.

We assume a two-level quantum system, having upper level $|2\rangle$ and lower level $|1\rangle$, which interacts with a resonant laser field

$$\vec{E}_x(z,t) = \vec{e}_x E_0 \cos(\Omega t - kz) , \tag{2.1}$$

polarized in the x direction and propagating along the z axis. This field undergoes laser frequency switching with the pulse sequence shown in Fig. 2 and produces a rotary echo. We seek solutions[12,13] of the density-matrix equations of motion

$$i\hbar \frac{\partial \rho}{\partial t} = [H, \rho] + (\text{damping terms}) , \tag{2.2}$$

where the Hamiltonian

$$H = H_0 + H'$$

consists of the free molecule term H_0 and the electric-dipole interaction

$$H' = -\vec{\mu} \cdot \vec{e}_x E_0 \cos(\Omega t - kz) .$$

For an optically thin sample of length L the transient signal field

$$E_{12}(z,t) = \tilde{E}_{12}(z,t) e^{i(\Omega t - kz)} + \text{c.c.} \tag{2.3}$$

obeys Maxwell's wave equation

$$\frac{\partial \tilde{E}_{12}}{\partial z} = -2\pi i k N \mu_{12} \langle \tilde{\rho}_{12} \rangle , \tag{2.4}$$

where the tilde denotes the slowly varying part and N is the molecular number density. The polarization

$$\langle \tilde{p}(t) \rangle = N \,\mathrm{Tr} \langle \mu \tilde{\rho}(t) \rangle \tag{2.5}$$

is to be averaged over the inhomogeneous line

shape, which is a Gaussian in the case of Doppler broadening. The angular brackets in (2.4) and (2.5) denote this average.

We introduce the phenomenological decay rates γ_1 and γ_2 to account for population loss from states $|1\rangle$ and $|2\rangle$, which are assumed to be in contact with a thermal reservoir. The rate γ_{21} describes radiative decay for the transition $|2\rangle \rightarrow |1\rangle$ and γ is the dipole-dephasing rate.

With the definition

$$\rho_{12}(z,t) = \tilde{\rho}_{12}(t) e^{i(\Omega t - kz)} \tag{2.6}$$

and the neglect of nonresonant terms, the equations of motion (2.2) become

$$\begin{aligned} \dot{\rho}_{11} &= \tfrac{1}{2} i\chi(\tilde{\rho}_{21} - \tilde{\rho}_{12}) - \gamma_1(\rho_{11} - \rho_{11}^0) + \gamma_{21}\rho_{22}\,, \\ \dot{\rho}_{22} &= \tfrac{1}{2} i\chi(\tilde{\rho}_{12} - \tilde{\rho}_{21}) - \gamma_2\rho_{22}\,, \\ \dot{\tilde{\rho}}_{12} &= \tfrac{1}{2} i\chi(\rho_{22} - \rho_{11}) + (-\gamma + i\Delta)\tilde{\rho}_{12}\,. \end{aligned} \tag{2.7}$$

Here the Rabi frequency χ, the tuning parameter Δ, and the eigenenergies E_i of the free molecule are given by

$$\chi \equiv \mu_{12} E_0/\hbar, \quad \Delta \equiv -\Omega + kv_z + \omega_{21}, \quad E_i \equiv \hbar\omega_i, \quad i = 1,2\,,$$

where kv_z is the Doppler shift and $\omega_{21} \equiv \omega_2 - \omega_1$.

As noted previously,[13] Eqs. (2.7) are not solved readily, since they involve four coupled equations in the variables ρ_{11}, ρ_{22}, ρ_{12}, and ρ_{21}, and therefore approximations are required. To make the problem tractable and yet retain the essential characteristics expected for optical rotary echoes, we restrict this discussion to two cases of damping:

$$\gamma_1 = \begin{cases} \gamma_2, & \gamma_{21} = 0 \\ 0, & \gamma_{21} = \gamma_2\,. \end{cases} \tag{2.8}$$

The first case corresponds to infrared molecular transitions where radiative decay can be neglected and the second to atomic ultraviolet transitions where only a few decay channels exist. In both cases there are only two decay parameters:

$$\gamma_2 = 1/T_1, \quad \gamma = 1/T_2\,, \tag{2.9}$$

making it possible to express (2.7) in terms of the Bloch equations:

$$\begin{aligned} &\dot{u} + \Delta v + \gamma u = 0\,, \\ &\dot{v} - \Delta u - \chi w + \gamma v = 0\,, \\ &\dot{w} + \gamma_2(w - w^0) + \chi v = 0\,. \end{aligned} \tag{2.10}$$

In (2.10) we have defined

$$u \equiv \tilde{\rho}_{12} + \tilde{\rho}_{21}, \quad v \equiv i(\tilde{\rho}_{21} - \tilde{\rho}_{12}), \quad w = \rho_{22} - \rho_{11}\,, \tag{2.11}$$

and $w^0 \equiv \rho_{22}^0 - \rho_{11}^0$ is the population difference at thermal equilibrium in the absence of the laser field.

B. Perturbative solutions

Solutions of Eqs. (2.10) are facilitated by application of the Laplace transform[4,13]:

$$\rho(z) = \int_0^\infty \rho(t) e^{-zt}\, dt\,,$$

$$z\rho(z) - \rho(0) = \int_0^\infty \dot{\rho}(t) e^{-zt}\, dt\,,$$

where $\rho(0)$ is the value at $t = 0$. The transformed equations of (2.10) in matrix form read

$$\begin{pmatrix} z+\gamma & \Delta & 0 \\ -\Delta & z+\gamma & -\chi \\ 0 & \chi & z+\gamma_2 \end{pmatrix} \begin{pmatrix} u(z) \\ v(z) \\ w(z) \end{pmatrix} = \begin{pmatrix} u(0) \\ v(0) \\ w(0) + (\gamma_2/z)w^0 \end{pmatrix}. \tag{2.12}$$

The inversion of (2.12) yields the solution

$$\begin{pmatrix} u(z) \\ v(z) \\ w(z) \end{pmatrix} = \frac{1}{D(z)} \begin{pmatrix} (z+\gamma)(z+\gamma_2) + \chi^2 & -\Delta(z+\gamma_2) & -\Delta\chi \\ \Delta(z+\gamma_2) & (z+\gamma)(z+\gamma_2) & \chi(z+\gamma) \\ -\Delta\chi & -\chi(z+\gamma) & (z+\gamma)^2 + \Delta^2 \end{pmatrix} \begin{pmatrix} u(0) \\ v(0) \\ w(0) + (\gamma_2/z)w_0 \end{pmatrix}, \tag{2.13}$$

where the matrix determinant

$$D(z) = (z+\gamma_2)[(z+\gamma)^2 + \Delta^2] + (z+\gamma)\chi^2\,. \tag{2.14}$$

The solution to $D(z) = 0$, which is a third-order equation in z, gives the three poles of the transformation needed to obtain u, v, and w. Rather than seek an exact solution to (2.14), which would be unnecessarily complex, we invoke the reasonable approximation that

$$\chi \gg \gamma, \gamma_2\,. \tag{2.15}$$

This condition means that many nutation cycles will appear in a dephasing time and of course is a desirable case for monitoring optical rotary echoes. Setting $\gamma = \gamma_2 = 0$ in (2.14), we find the zeroth-order solutions

$$z_1^{(0)} = 0, \quad z_{2,3}^{(0)} = \pm i\beta\,, \tag{2.16}$$

where the effective Rabi frequency

$$\beta = (\chi^2 + \Delta^2)^{1/2}\,.$$

To first order in γ/β, the first-order solutions

are

$$z_1^{(1)}=-\alpha_1,\quad z_2^{(1)}=i\beta-\alpha_2,\quad z_3^{(1)}=z_2^{(1)*}, \tag{2.17}$$

where

$$\alpha_1\equiv(\gamma_2\Delta^2+\gamma\chi^2)/\beta^2,\quad \alpha_2\equiv[\gamma\Delta^2+\tfrac{1}{2}(\gamma+\gamma_2)\chi^2]/\beta^2. \tag{2.18}$$

These roots are obtained by equating first-order terms in (2.14) with corresponding terms in the approximate relation

$$D(z)\cong(z-z_1^{(1)})(z-z_2^{(1)})(z-z_3^{(1)}).$$

Application of the inverse Laplace transformation

$$\rho(t)=\frac{1}{2\pi i}\int_{-i\infty+r}^{i\infty+r}e^{zt}\rho(z)dz \tag{2.19}$$

to (2.13), using the roots (2.17), yields the time-dependent behavior

$$\begin{aligned}
u(t)&=u(0)\left(\frac{\chi^2}{\beta^2}e^{-\alpha_1 t}+\frac{\Delta^2}{\beta^2}e^{-\alpha_2 t}\cos\beta t\right)-v(0)\frac{\Delta}{\beta}e^{-\alpha_2 t}\sin\beta t+w(0)\frac{\Delta\chi}{\beta^2}(-e^{-\alpha_1 t}+e^{-\alpha_2 t}\cos\beta t)+w^0\frac{\gamma_2\Delta\chi}{\alpha_1\beta^2}(e^{-\alpha_1 t}-1),\\
v(t)&=u(0)\frac{\Delta}{\beta}e^{-\alpha_2 t}\sin\beta t+v(0)e^{-\alpha_2 t}\cos\beta t+w(0)\frac{\chi}{\beta}e^{-\alpha_2 t}\sin\beta t+w^0\left(\frac{\gamma\gamma_2\chi}{\alpha_1\beta^2}+\frac{(\alpha_1-\gamma)\gamma_2\chi}{\alpha_1\beta^2}e^{-\alpha_1 t}-\frac{\gamma_2\chi}{\beta^2}e^{-\alpha_2 t}\cos\beta t\right),\\
w(t)&=u(0)\frac{\Delta\chi}{\beta^2}(-e^{-\alpha_1 t}+e^{-\alpha_2 t}\cos\beta t)-v(0)\frac{\chi}{\beta}e^{-\alpha_2 t}\sin\beta t+w(0)\left(\frac{\Delta^2}{\beta^2}e^{-\alpha_1 t}+\frac{\chi^2}{\beta^2}e^{-\alpha_2 t}\cos\beta t\right)\\
&\quad+w^0\left(\frac{\gamma_2\Delta^2}{\alpha_1\beta^2}(1-e^{-\alpha_1 t})+\frac{\gamma_2\chi^2}{\beta^3}e^{-\alpha_2 t}\sin\beta t\right).
\end{aligned} \tag{2.20}$$

Here we have consistently retained the leading terms in $u(0)$, $v(0)$, $w(0)$, and w^0. Note that these solutions[4] apply to optical nutation[14] or optical free induction decay[15] (with $\chi=0$), provided the above approximations are satisfied, and constitute the principal result of this section.

C. Rotary echoes

Armed with solutions (2.20), we can readily trace the evolution of the density-matrix element

$$\tilde\rho_{12}(t)=\tfrac{1}{2}[u(t)+iv(t)] \tag{2.21}$$

in accordance with the laser frequency switching pulse sequence of Fig. 2. To reiterate, at time $t=0$ the laser field is suddenly switched from $\Omega'\to\Omega$, thereby exciting a group of molecules which exhibits damped Rabi oscillations. The excitation is interrupted over the interval $T<t<T+\tau$ owing to the switch $\Omega\to\Omega'$, which introduces in time τ a phase shift

$$\phi=(\Omega'-\Omega)\tau \tag{2.22}$$

in the laser field. Rabi oscillations resume following the phase shift and the rotary echo appears at time $t=2T+\tau$.

Beginning at time $t=0$ the initial conditions $u(0)=0$, $v(0)=0$, $w(0)=-1$, and $w^0=-1$ allow us to evaluate (2.20) at $t=T$, namely,

$$\begin{aligned}
u(T)&=w^0\frac{\gamma_2\Delta\chi}{\alpha_1\beta^2}(e^{-\alpha_1 T}-1)+w(0)\frac{\Delta\chi}{\beta^2}(e^{-\alpha_2 T}\cos\beta T-e^{-\alpha_1 T}),\\
v(T)&=w(0)\frac{\chi}{\beta}e^{-\alpha_2 T}\sin\beta T,\\
w(T)&=w^0\frac{\gamma_2\Delta^2}{\alpha_1\beta^2}(1-e^{-\alpha_1 T})\\
&\quad+w(0)\left(\frac{\Delta^2}{\beta^2}e^{-\alpha_1 T}+\frac{\chi^2}{\beta^2}e^{-\alpha_2 T}\cos\beta T\right).
\end{aligned} \tag{2.23}$$

During the phase-interruption pulse, FID solutions follow from (2.20) by letting $\chi=0$. At $t=T+\tau$ we have

$$\begin{aligned}
u(T+\tau)&=u(T)e^{-\gamma\tau},\\
v(T+\tau)&=v(T)e^{-\gamma\tau},\\
w(T+\tau)&=w^0(1-e^{-\gamma_2\tau})+w(T)e^{-\gamma_2\tau}.
\end{aligned} \tag{2.24}$$

For the sake of simplicity we have introduced in (2.24) the approximation

$$\Delta\tau\ll 1, \tag{2.25}$$

which will apply for sufficiently brief pulses.

At $t=T+\tau$ the laser field has now acquired the phase shift (2.22), and therefore, for $t>T+\tau$, it is necessary to replace (2.1) by

$$\vec{E}_x(z,t)=\vec{e}_x E_0\cos(\Omega t+\phi-kz). \tag{2.26}$$

The equations of motion and the solutions are of the same form as (2.10) and (2.20) when we replace (2.6) by

$$\rho_{12}(z,t)=\tilde\rho'_{12}(t)e^{i(\Omega t+\phi-kz)}. \tag{2.27}$$

Thus in the new representation each off-diagonal density-matrix element is transformed according to

$$\tilde\rho'_{12}(t)=\tilde\rho_{12}(t)e^{-i\phi}. \tag{2.28}$$

For times $t>2T+\tau$ we retain only those terms in (2.20) that rephase at $t=2T+\tau$, i.e., echo terms are retained. The solutions now take the form

$$\begin{aligned}
u'_e(t)=e^{-\alpha_2(t-T-\tau)}\Big(&u'(T+\tau)\frac{\Delta^2}{\beta^2}\cos\beta(t-T-\tau)\\
&-v'(T+\tau)\frac{\Delta}{\beta}\sin\beta(t-T-\tau)\\
&+w(T+\tau)\frac{\Delta\chi}{\beta^2}\cos\beta(t-T-\tau)\Big),
\end{aligned}$$

$$v_e'(t) = e^{-\alpha_2(t-T-\tau)}\Big(u'(T+\tau)\,\frac{\Delta}{\beta}\,\sin\beta(t-T-\tau) + v'(T+\tau)\cos\beta(t-T-\tau) + w(T+\tau)\,\frac{\chi}{\beta}\,\sin\beta(t-T-\tau)\Big), \tag{2.29}$$

where the index e denotes "echo." It is apparent from (2.29) that we require the terms

$$u'(T+\tau) = \tfrac{1}{2}[u(T)+iv(T)]e^{-i\phi-\gamma\tau} + \text{c.c.},$$
$$v'(T+\tau) = (i/2)[u(T)-iv(T)]e^{i\phi-\gamma\tau} + \text{c.c.}, \tag{2.30}$$

which are easily derived from the definitions (2.11) using the transformation (2.28) and with the aid of (2.24).

A further simplification results if we allow the initial laser frequency to match the Doppler line center:

$$\Omega = \omega_{21}\,.$$

This condition causes the echo terms which are odd in the tuning parameter Δ to vanish upon integration of the echo signal over the Doppler line shape.

Inclusion of (2.23), (2.24), and (2.30) in (2.29) produces the resulting echo terms

$$u_e'(t) = 0\,,$$
$$v_e'(t) = w(0)(\chi^3/\beta^3)\sin\beta(t-2T-\tau)e^{-\alpha_2(t-\tau)-\gamma\tau} \times[\sin^2(\tfrac{1}{2}\phi) + \tfrac{1}{2}(e^{(\gamma-\gamma_2)\tau}-1)]\,, \tag{2.31}$$

which we see assume a remarkably simple form.

Now recall that the echo-field amplitude in a sample of length L is given by (2.3)–(2.5):

$$\tilde{E}_{12}^e(L,t) = -2\pi ikNL\,\mu_{12}\langle\tilde{\rho}_{12}^e(t)\rangle\,, \tag{2.32}$$

where the Doppler integral

$$\langle\tilde{\rho}_{12}^e(t)\rangle = \frac{1}{ku\sqrt{\pi}}\int_{-\infty}^{\infty}\tilde{\rho}_{12}^e(t)e^{-(\Delta/ku)^2}\,d\Delta\,, \tag{2.33}$$

u being the most probable molecular velocity. Expressing $\tilde{\rho}_{12}^e(t)$ in terms of (2.31), we find

$$\tilde{\rho}_{12}^e(t) = \tfrac{1}{2}e^{i\phi}[u_e'(t)+iv_e'(t)]$$

and the echo amplitude is

$$\tilde{E}_{12}^e(L,t) = (\sqrt{\pi}/u)NL\,\mu_{12}e^{i\phi}w(0)\chi^3e^{-\gamma\tau} \times[\sin^2(\tfrac{1}{2}\phi)+\tfrac{1}{2}(e^{(\gamma-\gamma_2)\tau}-1)] \times\int_{-\infty}^{\infty}\frac{\sin\beta(t-2T-\tau)}{\beta^3}\,e^{-\alpha_2(t-\tau)}e^{-(\Delta/ku)^2}\,d\Delta\,. \tag{2.34}$$

Since the phase-shifting pulse can be sufficiently brief that the decay will be insignificant, we can set $\gamma\tau \ll 1$ to obtain a slight simplification in (2.34). The final result is

$$\tilde{E}_{12}^e(L,t) = (\sqrt{\pi}/u)NL\,\mu_{12}e^{i\phi}w(0)\chi^3\sin^2(\tfrac{1}{2}\phi) \times\int_{-\infty}^{\infty}\frac{\sin\beta(t-2T-\tau)}{\beta^3}\,e^{-\alpha_2 t}e^{-(\Delta/ku)^2}\,d\Delta\,, \tag{2.35}$$

where

$$\alpha_2 = [\gamma\Delta^2 + \tfrac{1}{2}(\gamma+\gamma_2)\chi^2]/\beta^2\,.$$

It may be useful at this point to recall the assumptions and conditions which apply in obtaining (2.35), namely,

$$\chi \gg \gamma, \gamma_2, \quad \Delta\tau \ll 1 \text{ and } \gamma\tau \ll 1, \quad \Omega = \omega_{21}\,.$$

D. Characteristics

Before considering the Doppler integral in (2.35), which must be handled numerically, certain properties of (2.35) can be identified immediately. First the factor $e^{i\phi}$ merely indicates that the signal field is retarded in phase to the same extent that the driving field (2.26) is.

The $\sin^2(\frac{1}{2}\phi)$ factor in (2.35) supports (1.1) by revealing that the echo amplitude

$$\tilde{E}_{12}^e = \begin{cases} \text{a maximum}, & \phi = \pi, 3\pi, 5\pi, \ldots \\ 0, & \phi = 0, 2\pi, 4\pi, \ldots\,. \end{cases} \tag{2.36}$$

Hence the echo amplitude can be precisely controlled by adjusting the phase retardation ϕ. This precision is not ordinarily available with photon echoes,[16] unless $\chi \gg ku$, since the laser-field radial profile is Gaussian and hence the optical-pulse area assumes a continuous distribution of values. Furthermore, for a rotary echo each transition of a degenerate set will experience the same phase shift, independent of the distribution of transition-matrix elements.[7]

The $\sin\beta(t-2T-\tau)$ term of the integral shows that the echo appears at time $t = 2T+\tau$, at which point the signal vanishes: $\tilde{E}_{12}^e(t = 2T+\tau) = 0$.

A numerical calculation of the integral in (2.35) is shown in Fig. 3, which exhibits a damped Rabi oscillation with the expected crossing at the time origin. Numerical values of the parameters are given in the caption of Fig. 3. To understand the damping behavior, first note that the $1/\beta^3$ factor is sharply peaked about $\Delta = 0$, so that the principal part of the integral arises from the low-frequency components. This observation suggests the approximation

$$\alpha_2 \cong \tfrac{1}{2}(\gamma+\gamma_2)\,. \tag{2.37}$$

When (2.37) is included in (2.35), the dashed curve of Fig. 3 results. The close agreement in the two curves, particularly at long times, supports the approximation (2.37), which we now see is a valid description of the damping rate.

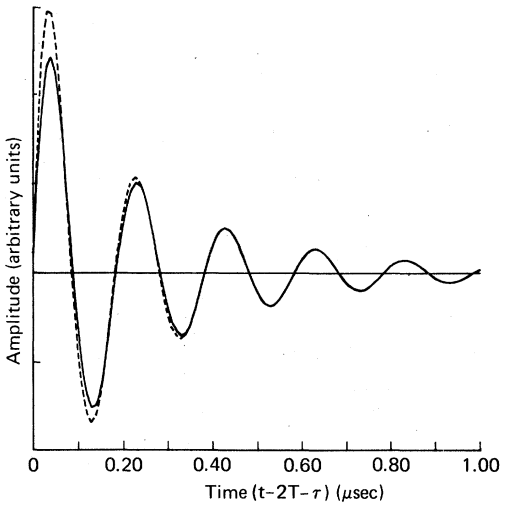

FIG. 3. Solid line is a computer plot of the rotary-echo solution of Eq. (2.35), while dashed line is one of the same solution using approximation Eq. (2.37), with $ku/2\pi = 500$ MHz, $\chi/2\pi = 5$ MHz, $\gamma = 3\,\mu\text{sec}^{-1}$, $\gamma_2 = 2\,\mu\text{sec}^{-1}$, $T = 1\,\mu$sec, and $\phi = \pi$.

Note that the damping rate (2.37) applies also in the strong-field limit, the NMR case,[1] where

$$\chi^2 \gg (ku)^2 .$$

This can be seen without numerical integration as α_2 reduces to Eq. (2.37) immediately. Therefore our results yield the same decay rate as Eq. (1.2), which is the original result derived by Solomon for NMR.

If we relax the restriction (2.8), we are still able to obtain the echo damping rate for arbitrary γ_1, γ_2, γ_{21}, and γ. Employing the perturbative method as described in Sec. II B, again assuming $\chi \gg \gamma_1, \gamma_2, \gamma_{21}, \gamma$, we see that Eq. (2.18) is replaced by

$$\alpha_2' = \{\gamma\Delta^2 + \tfrac{1}{2}[\gamma + \tfrac{1}{2}(\gamma_1 + \gamma_2 + \gamma_{21})]\chi^2\}/\beta^2 . \qquad (2.38)$$

Therefore the echo damping rate (2.37) becomes

$$\alpha_2' \cong \tfrac{1}{2}[\gamma + \tfrac{1}{2}(\gamma_1 + \gamma_2 + \gamma_{21})] . \qquad (2.39)$$

It is worth mentioning that rotary echoes arising from either an optical-field inhomogeneity or a Doppler-line-broadening inhomogeneity are not fundamentally different processes. This point is suggested in the effective Rabi-frequency parameter

$$\beta = (\chi^2 + \Delta^2)^{1/2} ,$$

where the Rabi frequency and the tuning parameter appear on an equal footing. Hence we expect that a distribution in either χ or Δ will lead to the same transient behavior, which the above analysis shows.

III. DETECTION OF ROTARY ECHOES

Rotary echoes are observed by the method of laser frequency switching.[10] A cw dye laser is frequency switched by an intracavity electro-optic phase modulator, an x-cut ammonium dideuterium phosphate crystal (AD*P) that is driven by a dc voltage pulse generator. The beam of this laser passes through a sample of I_2 vapor before striking a P-I-N diode photodetector (HP 5082-4227), where the transient signals are monitored with a 7904 Tektronix sampling oscilloscope and thereafter are displayed on an X-Y recorder.

The selected I_2 transition,

$$(v, J) = 2, 59 \rightarrow 15, 60 \text{ of } X'\Sigma_g^+ \rightarrow B^3\pi_{0+u},$$

falls in the visible region at 16 956.43 cm^{-1}, the wavelength being determined to $1/10^6$ or better by a digital wavemeter. The I_2 vapor is contained in an evacuated cell of 20 cm length having a thermoelectrically refrigerated cold finger for regulating the I_2 vapor pressure. Except for self-broadening studies, a 30 mTorr I_2 vapor pressure was maintained. A 580A Spectra-Physics dye laser (Rhodamine 6G) delivered to the sample cell ~30 mW in a collimated beam of 0.5 mm diameter. A laser frequency shift $(\Omega - \Omega')/2\pi \sim 30$ MHz resulted when a 50 V dc square-wave pulse, from a Hewlett-Packard 214A generator, was applied to the intracavity AD*P phase modulator. Additional detailes can be found elsewhere.[10]

A typical optical rotary echo is presented in Fig. 4 and, as we shall see, confirms our expectations. However, additional characteristics not discussed yet require explanation. First note that the frequency switch $(\Omega - \Omega')/2\pi = 30$ MHz is adequate for observing coherent transients, since it far exceeds the homogeneous width of ~3 MHz. Since the shift is much smaller than the I_2 Doppler width of 500 MHz, there will always be two relevant velocity packets, one which is resonant and one which is nonresonant with the laser field. Each packet will generate its own set of coherent transients throughout the pulse sequence. For example, the rotary echo arises from a packet which is nonresonant with the laser field for times $t < 0$ preceding the initial switch. This velocity group becomes resonant at $t = 0$, when the frequency switch takes place, exhibits nutation, and thereafter produces the nutation or rotary echo in the fashion already described.

The second velocity packet is resonant with the laser field for $t < 0$. It becomes nonresonant at $t = 0$ and exhibits FID. The switching pulse which commences at $t = T$ causes this packet to be excited resonantly and generates an FID or photon echo at $t = 2T + \tau$ (Fig. 5).

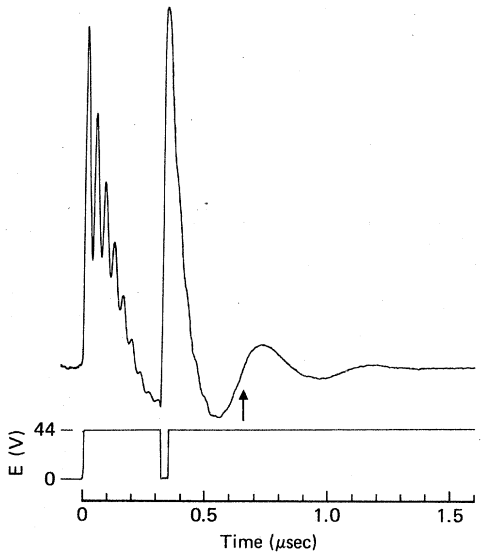

FIG. 4. Lower curve: dc voltage pulse sequence; upper curve: optical transient response of I_2, where arrow marks the rephasing point of rotary echo.

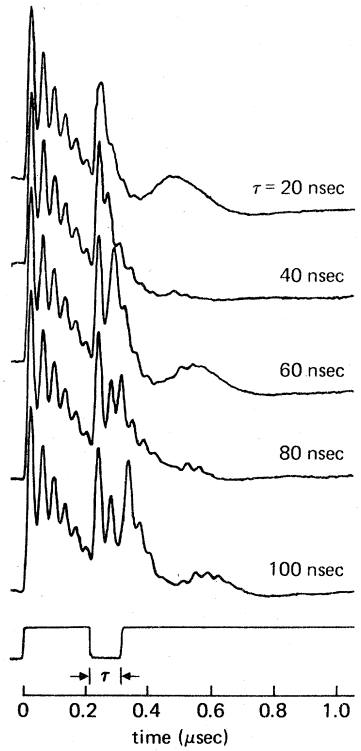

FIG. 5. Dependence of rotary-echo amplitude on pulse width τ. These measurements support the $\sin^2(\frac{1}{2}\phi)$ dependence of Eq. (2.35), where $\tau = 20$ nsec and a frequency shift of 26.7 MHz correspond to $\phi = 1.07\pi$.

Thus the rotary and photon echoes precisely overlap in time. They can be distinguished, however, because the shape functions are different. The rotary echo looks like a damped sinusoid where the oscillation frequency is $\sim\chi$, the Rabi frequency, and the FID echo displays a beat signal where the beat frequency is the shift $\Omega - \Omega'$. In addition, the FID echo can be suppressed by reducing the pulse width τ as in Fig. 4. The rotary echo can be suppressed by selecting a phase-interrupting pulse with $\phi = 0, 2\pi, 4\pi, \ldots$, as in Fig. 5. Finally, by switching completely outside the Doppler linewidth,[17] either rotary or photon echoes could be observed alone.

We wish to emphasize that optical rotary echoes will occur simultaneously with photon echoes in Stark or laser frequency switching whenever the frequency shift is less than the inhomogeneous linewidth. This point was not realized in previous studies.[9,10]

Now consider some of the other characteristics of the rotary echo which are revealed in Fig. 4. First the echo has the shape of a damped sinusoid which assumes a zero value at $t = 0.66$ μsec and resembles the theoretical result in Fig. 3. This crossing point identifies when the echo has rephased and agrees well with the predicted value $t = 2T + \tau = 0.64$ μsec, where the pulse delay time $T = 0.310$ μsec and the pulse width $\tau = 0.020$ μsec.

Preliminary studies of the rotary-echo damping

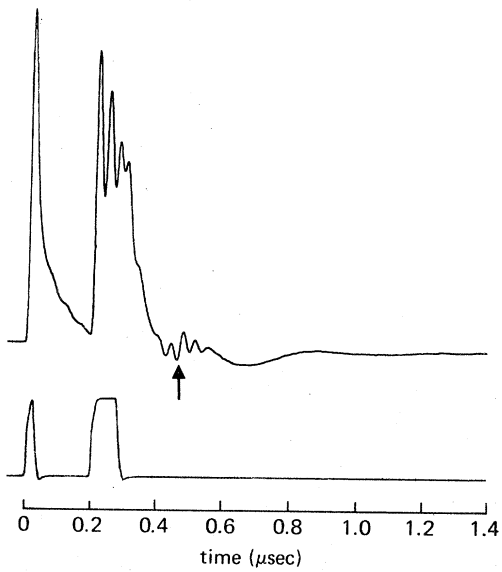

FIG. 6. Lower curve: dc voltage pulse sequence for two-pulse echo; upper curve: optical rotary and photon echoes superimposed, where arrow marks the rephasing point.

rate yield

$$\alpha = 0.63 + 0.051p(\text{mTorr})\,\mu\text{sec}^{-1}, \qquad (3.1)$$

where p is the I_2 vapor pressure, but it remains difficult at present to test the relation (2.37) or (2.39).

In Fig. 5 the rotary echo $\sin^2(\frac{1}{2}\phi)$ dependence in (2.35) is tested by varying the pulse width τ. For $\tau = 20$ nsec and a laser frequency shift $(\Omega - \Omega')/2\pi = 26.7$ MHz the phase retardation of the laser field $\phi = 1.07\pi$. Clearly the echo shape function is a maximum for odd multiples of π and tends to zero for even multiples of π, as predicted. Note that the accompanying photon echo which consists of small-amplitude, high-frequency oscillations (26.7 MHz) clustered about $t = 2T + \tau$ exhibits a different behavior with pulse width, which is well known.

Finally we have observed rotary (and photon) echoes, using a two-pulse laser frequency switching sequence (Fig. 6). Now the velocity packet which is excited resonantly in steady state for times $t < 0$ experiences an initial phase interruption arising from the first pulse. This procedure merely establishes an initial condition which differs from that used in Eq. (2.23). Thereafter the rotary-echo problem is precisely the same as the above treatment.

ACKNOWLEDGMENTS

This work was supported in part by the U. S. Office of Naval Research. One of us (N.C.W.) was supported by a Hertz Foundation Graduate fellowship.

[1]I. Solomon, Phys. Rev. Lett. 2, 301 (1959).
[2]E. L. Hahn, Phys. Rev. 80, 580 (1950).
[3]E. L. Hahn, Phys. Rev. 77, 297 (1950).
[4]H. C. Torrey, Phys. Rev. 76, 1059 (1949).
[5]F. Bloch, Phys. Rev. 70, 460 (1946).
[6]H. Y. Carr and E. M. Purcell, Phys. Rev. 94, 630 (1954).
[7]A. V. Nurmikko and S. E. Schwarz, Opt. Commun. 2, 416 (1971).
[8]F. Rohart, P. Glorieux, and B. Macke, J. Phys. B 10, 3835 (1977).
[9]R. G. Brewer and R. L. Shoemaker, Phys. Rev. Lett. 27, 631 (1971).
[10]R. G. Brewer and A. Z. Genack, Phys. Rev. Lett. 36, 959 (1976); A. Z. Genack and R. G. Brewer, Phys. Rev. A 17, 1463 (1978).
[11]A. Abragam, *The Principles of Nuclear Magnetism* (Oxford, London, 1961).
[12]R. G. Brewer, in *Frontiers in Laser Spectroscopy*, edited by R. Balian, S. Haroche, and S. Liberman (North-Holland, Amsterdam, 1977), p. 342.
[13]A. Schenzle and R. G. Brewer, Phys. Rev. A 14, 1756 (1976).
[14]G. B. Hocker and C. L. Tang, Phys. Rev. Lett. 21, 591 (1968); C. L. Tang and B. D. Silverman, in *Physics of Quantum Electronics*, edited by P. Kelley, B. Lax, and P. E. Tannenwald (McGraw-Hill, New York, 1966), p. 280.
[15]R. G. Brewer and R. L. Sheomaker, Phys. Rev. A 6, 2001 (1972).
[16]N. A. Kurnit, I. D. Abella, and S. R. Hartmann, Phys. Rev. Lett. 13, 567 (1964); I. D. Abella, N. A. Kurnit, and S. R. Hartmann, Phys. Rev. 141, 391 (1966).
[17]R. G. DeVoe and R. G. Brewer, Phys. Rev. Lett. 40, 862 (1978); Phys. Rev. A (in press).